Biomaterials 30 (2009) 4117–4126

Contents lists available at ScienceDirect

Biomaterials

journal homepage: www.elsevier.com/locate/biomaterials

A scaffold-bioreactor system for a tissue-engineered trachea

Chen-Huan Lin [a], Shan-hui Hsu [a,b,*], Chi-En Huang [a], Wen-Tung Cheng [a], Jang-Ming Su [c]

[a] Department of Chemical Engineering, National Chung Hsing University, Taichung, Taiwan, ROC
[b] Institute of Biomedical Engineering, National Chung Hsing University, Taichung, Taiwan, ROC
[c] Department of Surgery, Kuang Tien General Hospital Taichung, Taiwan, ROC

ARTICLE INFO

Article history:
Received 7 March 2009
Accepted 21 April 2009
Available online 17 May 2009

Keywords:
Tissue-engineering trachea
Bioreactor
Chondrocytes
Shear stress

ABSTRACT

A scaffold-bioreactor system was developed for growing tissue-engineered trachea and the effect of fluid flow on producing trachea-like neotissue was investigated. Chondrocytes were seeded in the poly (ε-caprolactone)-type II collagen scaffold and grown in the bioreactor operated under continuous flow at a rotational speed from 5 to 20 rpm. Flow analysis showed that the maximal and minimal shear stress in the bioreactor was 0.189–0.752 dyne/cm^2 and 30.3×10^{-5}–104×10^{-5} dyne/cm^2, respectively. After 4 and 8 weeks, the constructs were harvested from the bioreactor and analyzed. The application of rotation increased cell proliferation, GAG and collagen content in the constructs. Especially at 15 rpm, a two-fold increase in cell number, 170% increase in GAG, and 240% increase in collagen were found compared to static culture at 8 weeks. H&E staining showed the formation of neocartilage and the alignment of chondrocytes along the flow direction. The constructs grown under 15 rpm was selected for implantation into tracheal defects of rabbits. The mean survival of six animals was 52 days. The re-epithelialization of respiratory epithelium from the anastomotic sites was observed, with granulation tissue overgrowth. This successful initial step would allow us to make further improvement in applying tissue-engineering techniques to regenerate tracheas for practical use.

1. Introduction

Tracheal tissue is composed by chondrocytes, respiratory epithelial cells, collagen matrix, and blood vessels. The tracheal tube is reinforced by "C" shape cartilage that prevents collapse during inspiration. The surface of trachea is lined with functional ciliated respiratory epithelia. Researches in tracheal tissue engineering are mainly focused on two fields of interests: the tracheal cartilage reconstruction [1,2], and the lumen respiratory epithelialization [3,4]. One of the current challenges is to combine two different tissues, i.e. cartilage and epithelia, in tracheal tissue engineering. Kojima et al. made a non-woven poly(glycolic acid) fiber wrapped up silicone tube, with the inner and outer surface of the tube seeded with epithelial cells and chondrocytes, respectively. After implantation into the subcutaneous space of nude mice, the matrix components of the graft showed similarity to those of native tracheal tissue [5]. However, the graft collapsed only 7 days after implantation to sheep cervical trachea [6]. In a recent clinical study by Macchiarini et al., autologous epithelial cells and mesenchymal stem cells derived chondrocytes were seeded to human donor trachea and cultured in a rotational bioreactor. The graft provided the recipient a functional airway in the left bronchus at 4 months [7]. Despite using autologous tissue or tracheal allograft, each construct seems to have its own limitation. For example, the patients receiving donor trachea might require immunosuppressive therapy. Another important concern is the mechanical properties of tissue-engineering trachea, which are still far from satisfactory. To overcome the limitation of mechanical properties in tissue-engineering trachea, a poly(ε-caprolactone) (PCL)–collagen tracheal scaffold has been developed in our lab [8]. We showed that this composite scaffold could sustain mechanical strength. Besides, the scaffold was highly porous with type II collagen sponge filled in the multi-ring structure which provided a proper environment for the proliferation of chondrocytes.

Bioreactors are important tools for culturing long-segment tracheal tissue for clinical applications. As mentioned, in a recent clinical study human donor trachea seeded with autologous cells was cultured in a self-designed rotational bioreactor [7]. However, this study and other studies have not focused on hydrodynamic environment in tracheal tissue engineering. Dynamic culture systems can offer several important advantages compared with the static ones. For instance, mass transfer can be enhanced by

* Corresponding author. Department of Chemical Engineering, National Chung Hsing University, Taichung 40227, Taiwan, ROC. Tel.: +886 4 2284 0510x711; fax: +886 4 2285 4734.
E-mail address: shhsu@dragon.nchu.edu.tw (S.-h. Hsu).

0142-9612/$ – see front matter © 2009 Elsevier Ltd. All rights reserved.
doi:10.1016/j.biomaterials.2009.04.028

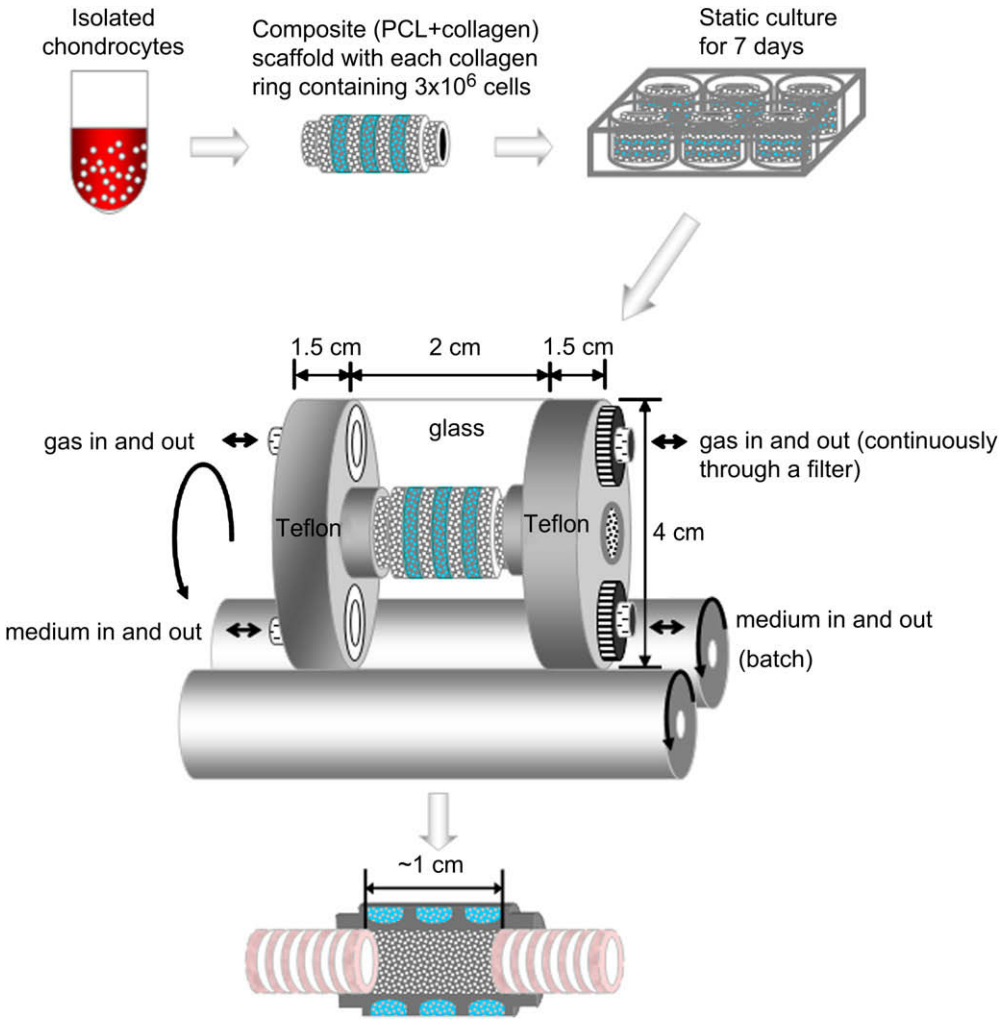

Fig. 1. A schematic diagram of the experimental design. Isolated cells were seeded on tracheal scaffolds, cultured statically in 6-well culture plates for 7 days and then transferred to the self-designed bioreactor system rotated in four different speeds (5, 10, 15 and 20 rpm).

convective fluid flow. In addition, physiologically relevant physical signals provided by a dynamic system, such as shear stress, compression, pressure, and stretch, can have influences on tissue development. Several studies have demonstrated that shear stress regulates the metabolism of ECM in tissue-engineered cartilage [9–12]. Since chondrocytes in vivo typically reside in a mechanically dynamic environment, the dynamic environment generated by a bioreactor is believed to provide an opportunity for

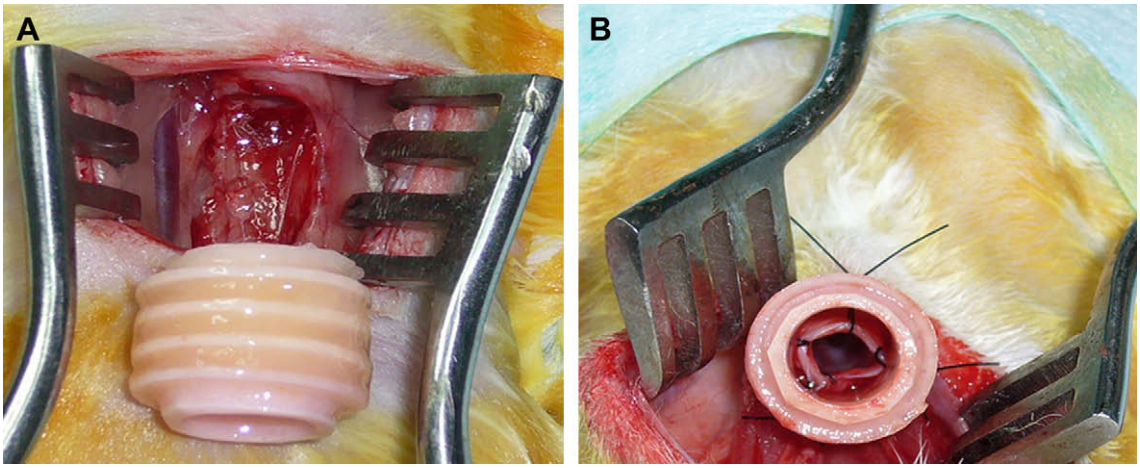

Fig. 2. Implantation of the PCL–collagen construct as a tracheal graft in rabbits. (A) The trachea defect (approximately 1 cm in length) is shown and (B) the PCL–collagen graft was implanted to the rabbit by telescopy anastomoses.

Table 1
Shear stresses across the construct surface obtained by the theoretical simulation in the self-designed rotating bioreactor (shown in Fig. 1).

Shear stress (dyne/cm^2)	5 rpm	10 rpm	15 rpm	20 rpm
Minimum	0.000303	0.000563	0.000835	0.00104
Maximum	0.189	0.360	0.544	0.752

reconstruction of larger tracheal constructs. A wide variety of bioreactor types have been developed for tissue engineering, such as spinner flasks [13], rotating wall vessels [14], concentric cylinders [15–17], and the perfusion system [18]. Each of these bioreactors provides a different flow stream and shear stress. Cartilage tissue grown in rotational bioreactors has been reported to be functionally more superior to that in static or in spinner flasks [19].

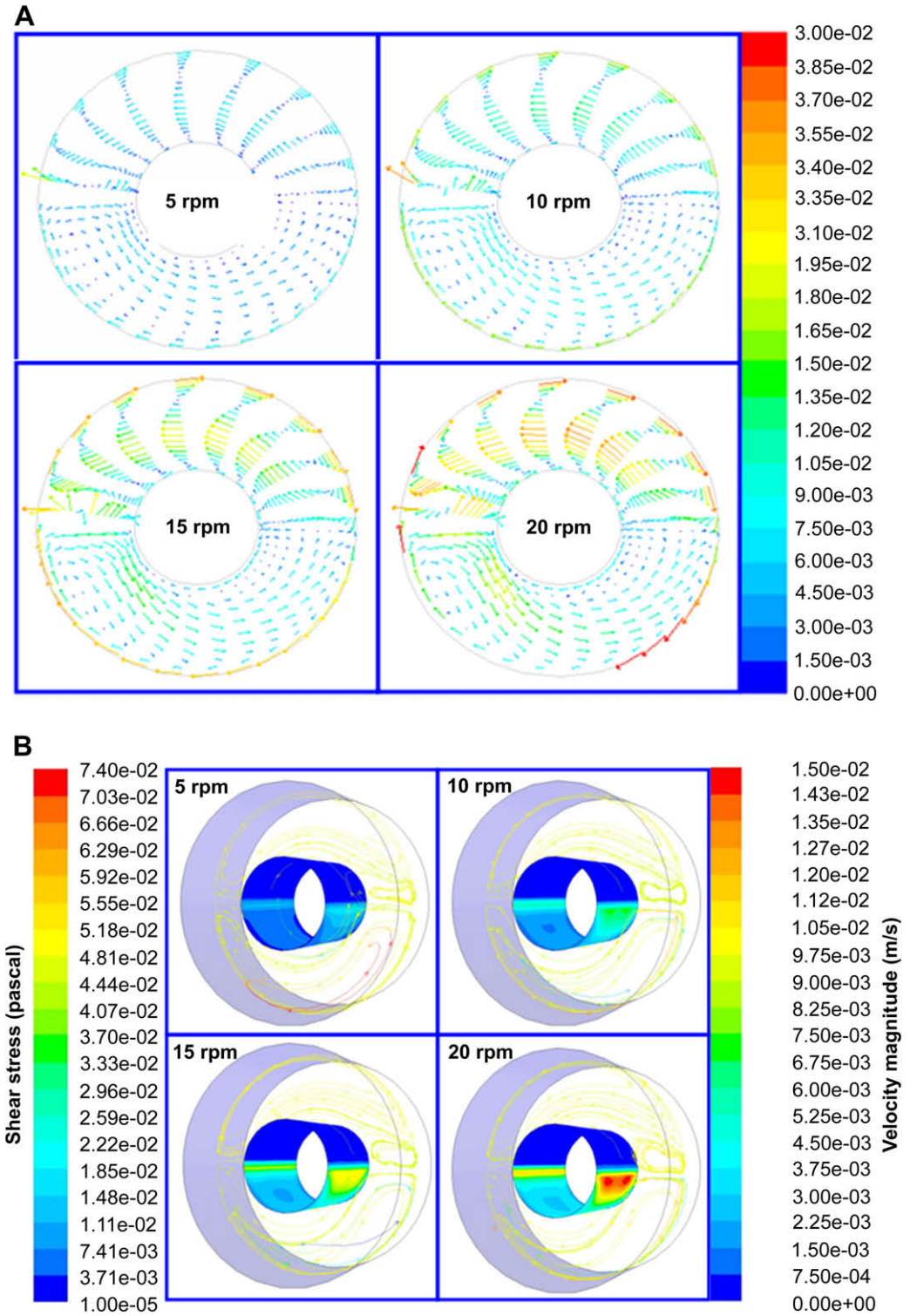

Fig. 3. Simulation results for: (A) the mean velocity vectors in the bioreactor at different rotational speeds; (B) the distribution of velocity magnitude and shear stress across the construct surface at different rotational speeds (1 Pa = 10 dyne/cm^2).

This might be due to the turbulent flow and higher shear stress created by the spinner flasks compared to the rotational bioreactor, which has predominately laminar flow conditions and lower shear stress.

In the current study, a rotational bioreactor was developed for the uniform production of tissue-engineering trachea. Constructs with the optimal growth condition were then implanted into rabbit cervical tracheal defects. Postoperative evaluation was conducted using flexible bronchoscopy and histological analyses. We expected that by combining tracheal tissue engineering and telescopic anastomosis technology, the lumen surface of the constructs could be epithelialized at an early stage of the healing process after implantation.

2. Materials and methods

2.1. Preparation of the tracheal scaffold

The tracheal composite scaffold (a grooved PCL stent in combination with ring-like type II collagen sponge in a tubular design) was fabricated as previously described [8]. Briefly, the stent part of the tracheal scaffold was prepared from 11% (w/v) 1,4-dioxane solution of PCL ($M_n = 80$ kDa, Aldrich, Milwaukee, WI, USA). The polymer solution was poured into a mold with special groove design and subsequently frozen at a temperature −20 °C for 8 h and then freeze-dried for 48 h to form the porous structure. Type II collagen was extracted from porcine costal cartilage using limited pepsin digestion [20]. The dried porous PCL grooved stent was immersed into 1% (w/v) type II collagen solution and subsequently frozen, so that the frozen type II collagen filled in the grooves and formed ring-like structure. The combination was freeze-dried for another 48 h. Then the collagen rings on the composite scaffold were crosslinked by 1% 1-(3-dimethyl aminopropyl)-3-ethyl-carbodiimide hydrochloride (EDC, Lancaster, Alfa Aesar, UK) and then soaked in distilled water for 24 h after washing with distilled water several times. The scaffold was then dried in vacuum for 24 h and stored at −20 °C until use.

2.2. Bioreactor configurations

The self-designed bioreactor is shown in Fig. 1. The rotation wall vessel bioreactor was comprised of a glass cylindrical chamber (inner diameter = 3.5 cm, length = 5 cm) with two extremities sealed by Teflon caps. A Teflon membrane filter (0.22 μm, Pall, USA) was placed on each hole of the Teflon caps intended for the gas exchange and medium change. The construct was placed on the holder in the glass chamber. The vessel contained 10 ml of culture medium in the chamber and was operated horizontally by rotation at a rate of 5, 10, 15 or 20 rpm on a roller deck. To sterilize the bioreactor, the vessels and caps were autoclaved together.

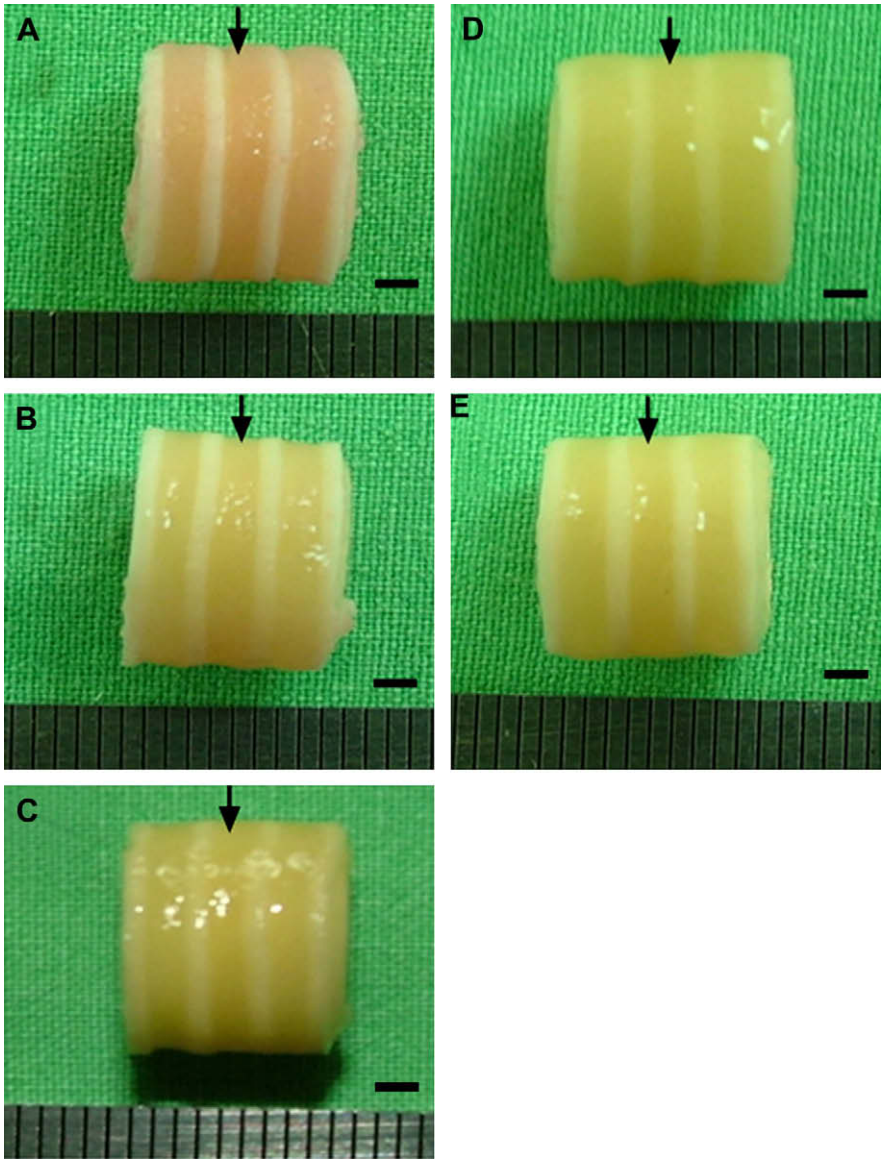

Fig. 4. The photographs of 8 week constructs cultured in the bioreactor at different speeds: (A) static; (B) 5 rpm; (C) 10 rpm; (D) 15 rpm; (E) 20 rpm. Arrows indicate the region of cartilage regeneration (scale bar: 2 mm).

2.3. Analysis of flow behavior within the bioreactor through computational fluid dynamics (CFD)

The shear stresses exerting on the surface of the scaffold were calculated directly by FLUENT software (Fluent Corp., Lebanon) for various rotating speeds. The mathematical computation of shear stress profiles in a bioreactor was simulated by computational fluid dynamics (CFD) modeling. The geometry of the bioreactor with meshes was created by Gambit software (Fluent Corp., Lebanon). After suitable boundary conditions were defined, the mesh file was then associated for calculation. The flow field of liquid and air could be visualized by the post processing tools for analysis of flow behavior within the bioreactor.

Considering the simple rotation mechanism of the bioreactor filled with half liquid medium, a volume of fluid (VOF) model was used to handle the liquid and gas phase interface to perform the individual flow phenomenon in each cell throughout the computation domain. The model of liquid–air interface was set as unsteady state. Additionally, a monitor point was set to confirm the flow fields as a pseudo-steady state. The entire reactor was rotated at a fixed rotational rate set in wall boundary condition panel. Four different rotational speeds 5, 10, 15, and 20 rpm were performed in this study.

2.4. Isolation of chondrocytes from rabbits

The cartilage was collected from the articular joint of male New Zealand white rabbits (weighing about 1–2 kg, 60 days of age) and then chondrocytes were isolated by sequential digestion with hyaluronidase, 0.2% trypsin, and type II collagenase [21]. Primarily cultured rabbit chondrocytes were maintained in Dulbecco's modified Eagle's medium (DMEM) (Gibco/BRL, Grand Island, NY, USA) containing 10% fetal bovine serum (Biological Industries, Beit Haemek, Israel), 1% penicillin–streptomycin–amphotericin B solution, and 44 mM $NaHCO_3$. Cultures were incubated in a humidified incubator with 5% CO_2 at 37 °C. At confluence (approximately 10 days), chondrocytes were trypsinized and suspended to create a single cell suspension. 0.1 ml of the chondrocyte suspension (3×10^7 cells/ml) was dropped onto each collagen ring of the tracheal scaffold. Each scaffold was then placed into the well of a 6-well plate and maintained in an incubator for three days. Medium was refreshed every day. After the pre-culture, tracheal scaffolds were transferred to the rotational bioreactor described above. Static control remained in the 6-well plate and the media were refreshed every day. Specimens were terminated at 4 and 8 weeks for biochemical assays and histological analyses.

2.5. Biochemical assays

The cellularity of tracheal constructs was determined by analyzing the DNA content [22]. The fluorescent dye Hoechst 33258 (0.1 g/ml) was added to papain-digested solution and fluorescence was measured immediately at room temperature by a fluorescence spectrophotometer (Hitachi F2500, Japan), with excitation at 365 nm and emission at 458 nm.

The glycosaminoglycan (GAG) content was determined by dimethylmethylene blue (DMMB, Aldrich) [23]. Briefly, DMMB solution was added to 100 μl aliquot of papain-digested solution and measured by a UV/VIS spectrophotometer (Hitachi U-2000, Japan) with an absorbance at 525 nm.

The amount of collagen was quantified by an indirect method of the presence of the collagen-specific amino acid hydroxyproline after reaction with *p*-dimethylamino-benzaldehyde and was quantified by an ELISA reader (Molecular Device, USA) [24].

2.6. Animals and operative techniques

Experiments were performed on adult rabbits ($n = 6$, weighing about 1–2 kg, 60 days of age). Rabbits were anesthetized intramuscularly with ketamine hydrochloride (1 ml/kg) and xylazine hydrochloride (Rompun, 0.2 ml/kg). The PCL–collagen graft grown in the bioreactor at 15 rpm for 8 weeks was implanted to the 1 cm tracheal defect in each rabbit (Fig. 2A, B) and the defect was sutured by the telescopic anastomosis technique using continuous sutures (4-0 Monosof). All procedures followed the guidelines for the animal care, and the Ethical Committee of National Chung Hsing University had approved the experiment.

2.7. Postoperative observations

The incorporation of implanted tissue-engineered trachea with host tissue and the lumen stenosis was observed by a bronchoscope (GIMMI GmbH, Tuttlingen, Germany) at 3 and 28 days. The narrowest section of the airway lumen at each time point was measured. The animals were euthanized and the tracheal specimens were harvested for histological evaluation.

2.8. Histological examination

For histological examination, the in vitro tissue-engineering tracheal constructs or the explanted grafts were fixed in 10% neutral buffered formalin, embedded in paraffin wax, and thin-sectioned (3 μm). The sections were stained with hematoxylin & eosin (H&E) for cell morphology and safranin-O for the presence of GAG. For immunohistochemcal evaluation, sections were stained with a type II collagen antibody (Neomarkers, USA) and visualized via DAB staining (Immunotech, France) according to the manufacturer's protocol. Sections were observed by an optical microscope (Nikon Eclipse 80i, Japan).

2.9. Statistical analysis

Statistical differences were analyzed by one-way analysis of variance (ANOVA). $p < 0.05$ was considered statistically significant. The data were expressed as mean ± standard deviation ($n = 3$).

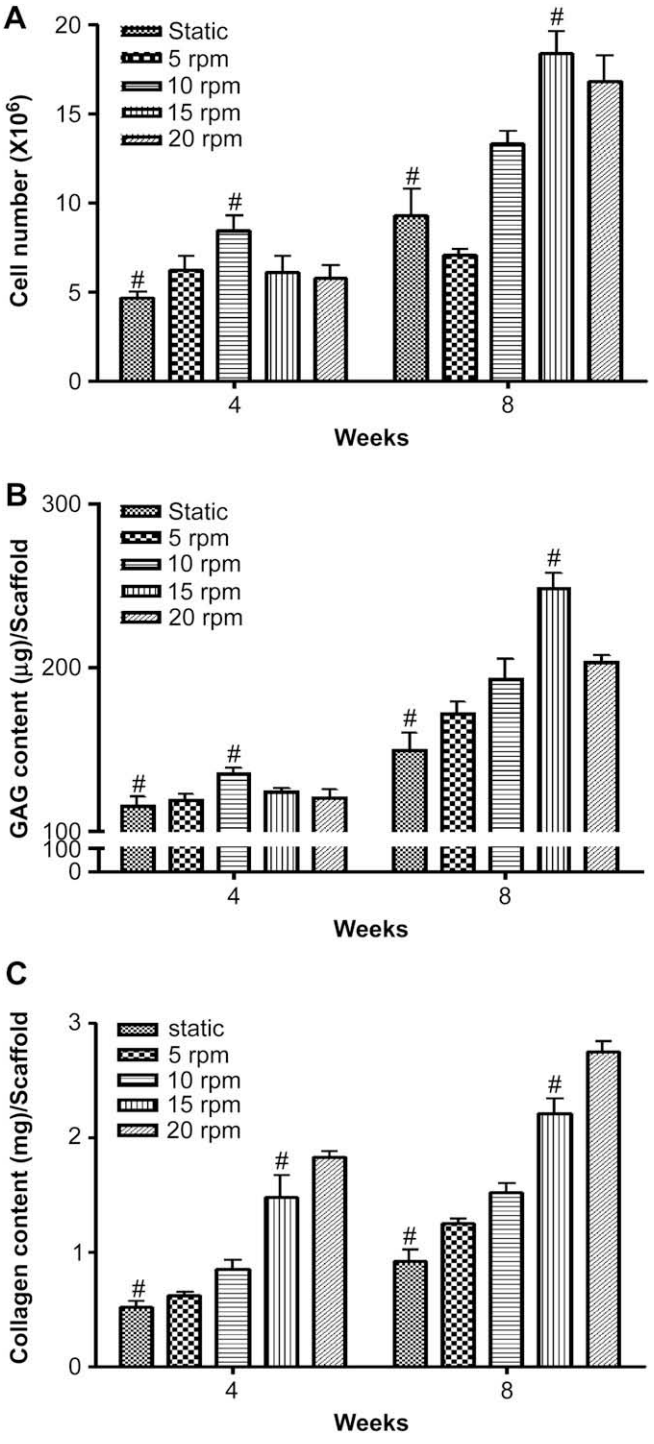

Fig. 5. The effect of rotational speed on chondrocyte proliferation and matrix deposition: (A) the number of cells and the amount of (B) GAG and (C) collagen. #$p < 0.05$ ($n = 3$; compared with static).

3. Results

3.1. Flow simulation

The rotational bioreactor was operated under continuous flow at a rotational speed of 5, 10, 15 or 20 rpm. The medium (~10 ml) was approximately half full of the glass chamber during the culture period. Based on the simulation, the fluid flow at the construct surface was laminar. The maximal shear stresses were between 0.189 and 0.752 dyne/cm^2 and minimal shear stresses were between 30.3×10^{-5} and 104×10^{-5} dyne/cm^2 at different rotational speeds (Table 1). Fig. 3A shows vertical cross-sections of

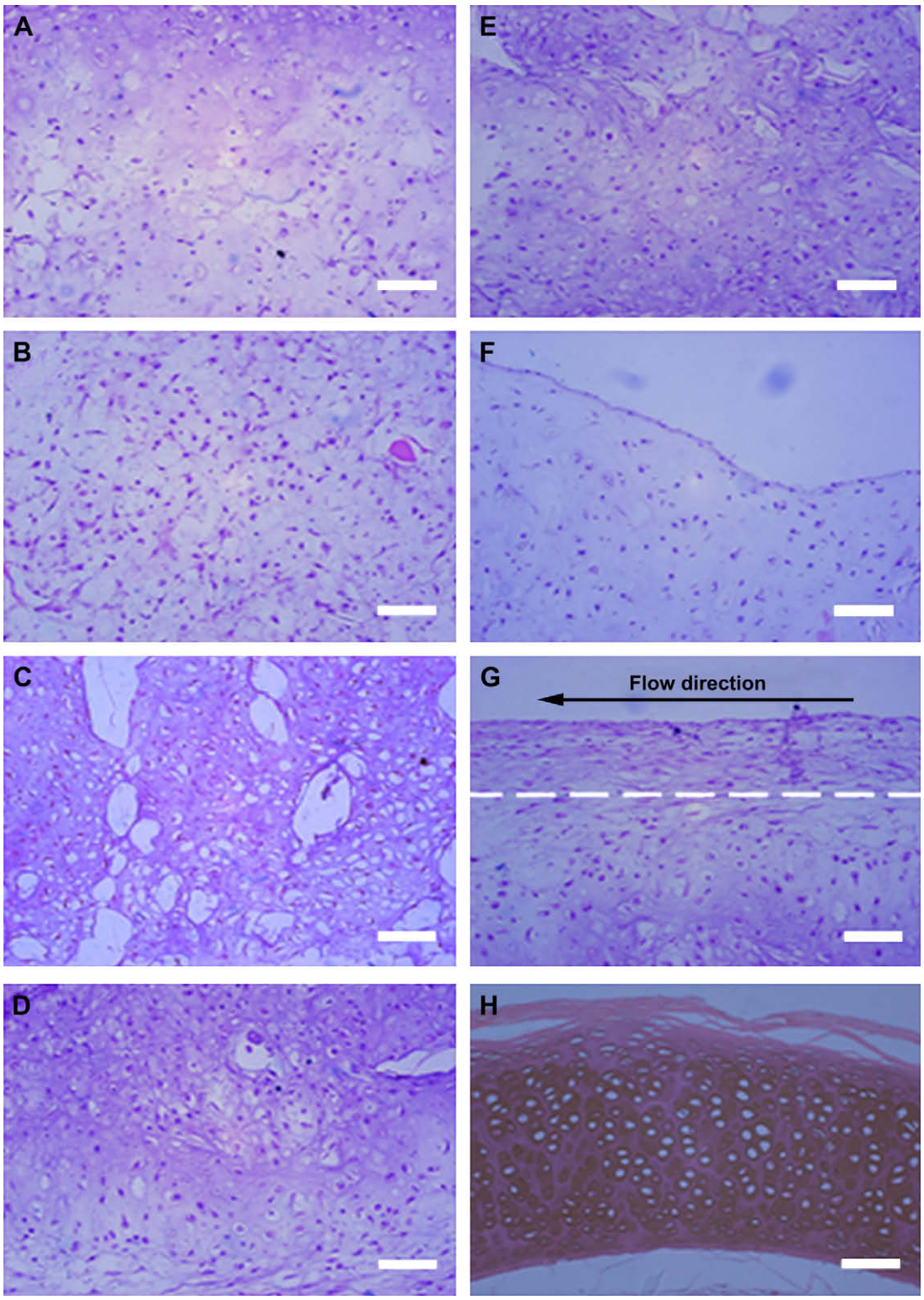

Fig. 6. H&E stained sections of the interior region (A–E) and edge region (F, G) for PCL–collagen constructs incubated for 8 weeks under varying culture conditions: (A) static; (B) 5 rpm; (C) 10 rpm; (D) 15 rpm; (E) 20 rpm. The histology of native trachea is also show in (H) (scale bar: 100 μm).

velocity vector at different speeds. The color of the arrows represents the velocity magnitude in the plane, ranging from zero (dark blue) to the maximum at the outside wall (red). The shear stress field at an instant of time in the construct surface at different rotational speeds is illustrated in Fig. 3B. The shear stress was concentrated along the construct surface, near the air–liquid interface. The shear stresses at the construct surface increased when the rotational speed increased. Especially, a large gradient of

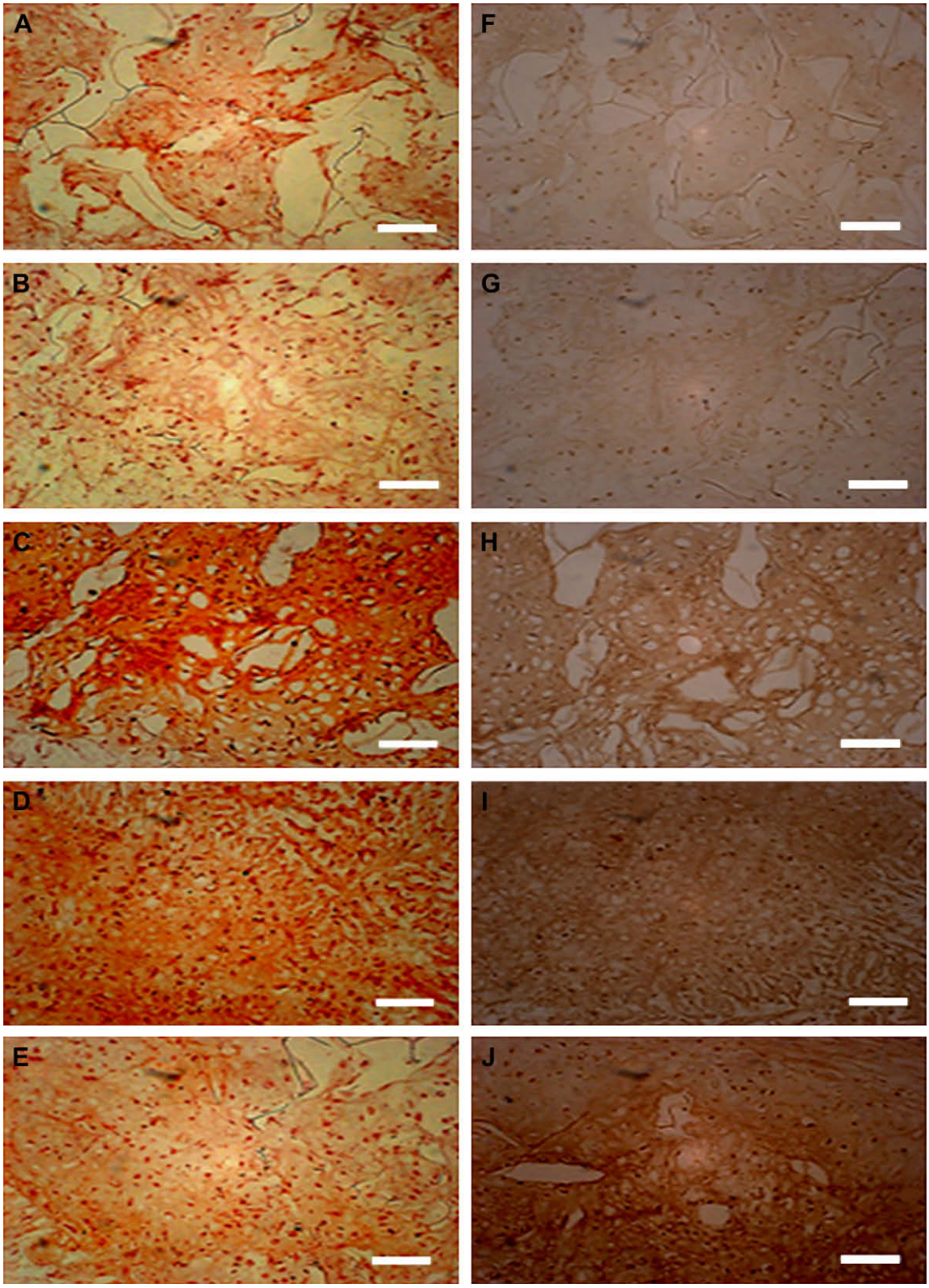

Fig. 7. Safranin-O (A–E) and immunohistochemical type II collagen (F–J) stained sections of PCL–collagen constructs incubated for 8 weeks under varying conditions: (A, F) static; (B, G) 5 rpm; (C, H) 10 rpm; (D, I) 15 rpm; (E, J) 20 rpm (scale bar: 100 μm).

the shear stress was produced along the edge at the speed of 20 rpm.

3.2. Macroscopic appearance and the biochemical assays of constructs cultured in vitro

After 8 weeks, the constructs had pink colored surface in static culture (Fig. 4A). The constructs harvested from bioreactors showed yellowish glistening surface that resembled the macroscopic appearance and shape of cartilaginous tissue (Fig. 4B–E). Cell number was higher for the constructs cultured in bioreactors than that in static culture (Fig. 5A), and was highest for those cultured at 10 rpm (for 4 weeks) and at 15 rpm (for 8 weeks). The GAG content of the constructs followed a similar trend as cell number (Fig. 5B). The collagen content of the constructs in bioreactors was superior to that in static culture (Fig. 5C). In general, bioreactors rotated at 15 rpm gave the best results.

3.3. Histological analyses of constructs cultured in vitro

The organization of chondrocytes in static and dynamic conditions is shown in Fig. 6A–E. The chondrocytes cultured statically appeared to be randomly distributed with no orientation (Fig. 6F), whereas chondrocytes cultured in 15 rpm were well organized and aligned along the direction of medium flow (Fig. 6G), with the morphology similar to the native trachea tissue (Fig. 6H). Moreover, the morphology of cells was spindle on the surface of the construct but was round and regularly oriented cells inside the construct. GAG deposition was higher in dynamic culture (Fig. 7B–E) than in static culture (Fig. 7A). Especially, GAG deposition was more intense and uniformly distributed in constructs cultured at the rotational speed of 15 rpm compared to other speeds. Fig. 7F–J shows the immunohistochemical staining of collagen type II. The staining intensity of collagen type II at 8 weeks was more intense for the constructs grown in the bioreactor than those in static. Unlike the other two parameters (cell number and GAG), the collagen type II deposition increased with the increase in rotational speed.

3.4. Bronchoscopic examination and histological analyses in vivo

The postoperative examination for rabbits revealed that the constructs were neither infected nor collapsed after implantation for 3 days (Fig. 8A). After 28 days, the interior surface of the constructs was covered with a layer soft tissue (as indicated by the arrow) (Fig. 8B). All animals were sacrificed as a result of airway stenosis. Animal survival time ranged from 43 to 81 days (Table 2). After implantation for 43 days, granulation tissues continued from the proximal to the distal anastomotic sites (as indicated by the circle in Fig. 9A) and were interspersed with numerous blood vessels. In the interior of the scaffolds, pores were completely infiltrated with connective tissue (as indicated by the arrow in Fig. 9B). Fig. 9B shows the high magnification images of granulation tissue with blood vessels indicated by the arrows. Re-epithelialization of respiratory epithelium from the anastomotic sites overlying a layer of connective tissue (as indicated by the arrow) is shown in Fig. 9C.

4. Discussion

Bioreactors play an important role in tissue engineering, because the fluid flow in bioreactors can enhance nutrient mass transfer and stimulate cell proliferation and matrix secretion [25]. Although different bioreactors were designed for applications to cartilage [26], bone [27,28], skin [29], or blood vessel [30] tissue engineering, those for trachea tissue engineering have not been developed in detail. By moving cells between liquid (medium) and gaseous (air) phases, bioreactors provide an environment for better attachment of implanted cells to the constructs and matrix formation for engineering larger tracheal segments [7]. However, limited researches have focused on characterizing the hydro dynamic environment or quantifying the associated shear stress.

Shear stress plays an important role in regulating cell function. Smith et al. reported that fluid shear stress caused morphological changes in articular chondrocytes and induced the release of soluble mediators and extracellular matrix macromolecules [31,32]. Our results showed that chondrocytes were well organized and aligned along the flow direction under single-direction of fluid flow and achieved morphology similar to that of native trachea tissue. Regarding the values of shear stress in different kinds of bioreactors for tissue-engineering cartilage, 1.1 dyne/cm^2 was estimated for spinner flasks [13], 0–0.32 dyne/cm^2 was obtained for a 10 rpm rotating-shaft bioreactor [33], and 1.5–12 dyne/cm^2 was calculated for concentric cylinder bioreactors [15,16]. The shear stress of the constructs was from 0.189 to 0.752 dyne/cm^2 by CFD simulation in our system. At 8 weeks, it was also found that at 15 rpm (maximum shear stress 0.544 dyne/cm^2) the synthesis of type II collagen and

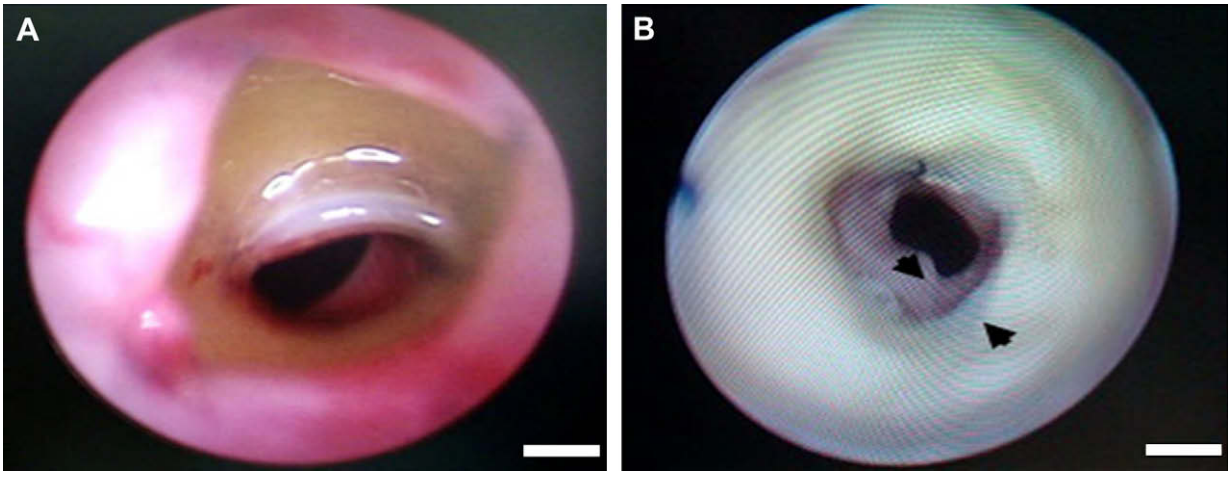

Fig. 8. The bronchoscopic images for the tissue-engineered trachea implanted to the rabbits at different periods: (A) 3 days after implantation, the tissue-engineered trachea was intact and did not collapse; (B) a 28 days after implantation, the lumen surface showed granulation tissue formation (scale bar: 2 mm).

Table 2
Postoperative survival and tracheal status of tissue-engineered trachea implanted to rabbits.

No.	Survival time (d)	Tracheal status	Lumen dimension (mm)
1	45		2
2	49		1
3	53	Granulation tissue overgrowth and induced airway stenosis	2
4	81		1
5	43		3
6	43		3

GAG increased 240% and 170%, respectively, compared to the static control. Although GAG level increased with rotation speed, the concentration of GAG was significantly less at the rotation speed of 20 rpm, while the concentration of type II collagen increased with the rotation speed. Gemmiti et al. have developed a parallel-plate bioreactor with shear stress about 1 dyne/cm^2 where the fluid flow enhanced the mass transport and type II collagen deposition compared to the static control [34]. It was speculated that high shear stresses enhanced the ability of chondrocytes-mediated deposition of type II collagen to counteract the shear force. Overall, our results showed that the air–liquid bioreactor provided essential oxygen and nutrient transport between the chondrocytes and the culture media, as well as the mechanical stimuli necessary to promote ECM synthesis. Macroscopic appearance of the tissue-engineering tracheal constructs cultured in our rotational bioreactor revealed cartilage-like tissue at 8 weeks. Unlike the constructs made from a non-woven PGA fiber wrapped silicone tube seeded with chondrocytes that survived only 7 days after implantation [6], our results showed that the PCL–type II collagen scaffold seeded with chondrocytes was able to maintain structural integrity when implanted to the rabbit cervical trachea defect. The grafts maintained the original structure without collapse or air leakage in vivo and the average survival time in six animals was 52 days. These results indicated that PCL stent provided adequate mechanical strength to serve as a proper scaffold for trachea tissue engineering.

Among the methods for tracheal reconstruction, end-to-end anastomosis has the drawback of leakage and local infection after implantation. In addition, the vessel ingrowth in the interior of the graft was too slow to provide adequate nutrient to respiratory epithelial cells. Telescopy anastomoses technique was chosen in this study for tracheal reconstruction mainly because of the rapid formation of granulation tissue that has the ability to enhance vascularization and the survival of epithelial cells. Although the granulation tissues in the tracheal lumen might guide the migration of epithelial cells into the middle site of the lumen from the two anastomoses, stenosis of the airway could be led by overgrowth of granulation tissue. To improve tissue healing and reduce airway stenosis in a tracheal graft, several strategies have been developed, such as surface modification of the graft and cell seeding to the lumen of the graft. Sondrup et al. reported that polyvinylchloride tubular stents coated with a crosslinked derivative of hyaluronan could prevent stenosis [35]. Polypropylene spiral tracheal prostheses sealed with collagen sponges could promote tissue regeneration and overcame stenosis [36]. Chitosan–gelatin hydrogel as

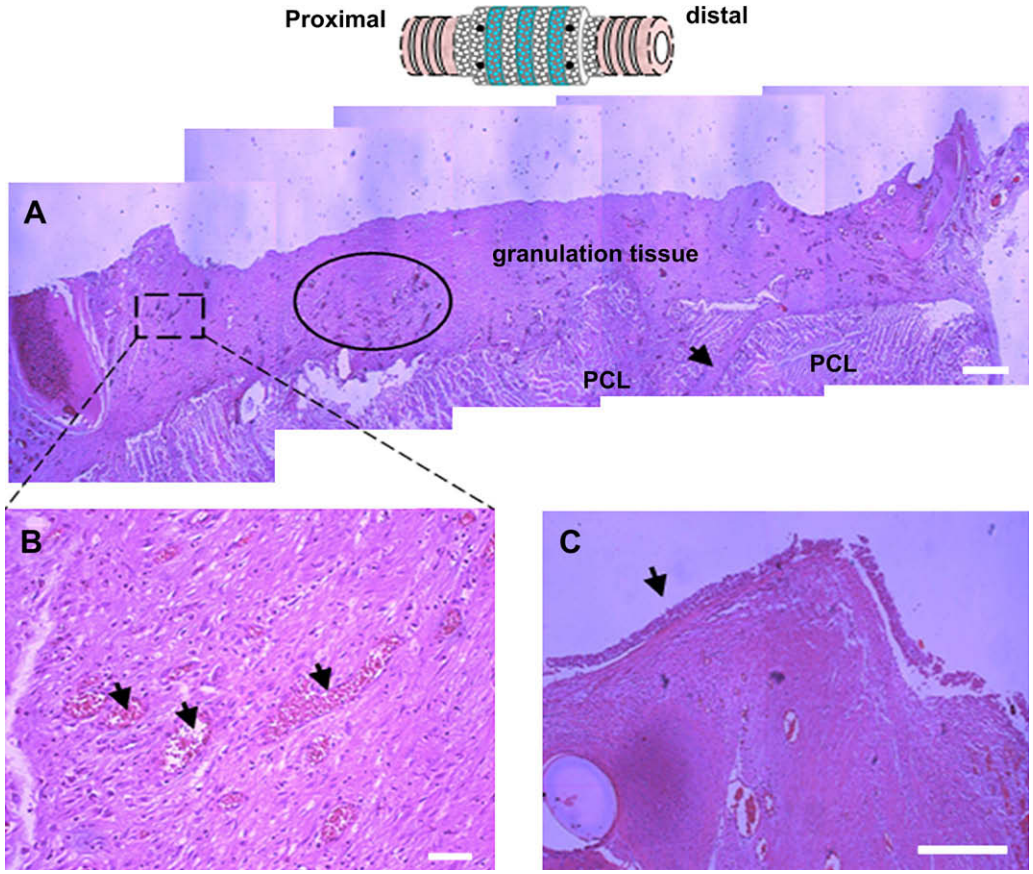

Fig. 9. H&E stained explants showing (A) lengthwise section of airway in the regenerated site at 43 days after operation where a layer of connective tissue overlying anastomotic sites with numerous blood vessels (indicated by the circle) was observed; (B) magnification of dotted area in (A); (C) the lumen surface re-epithelialized (indicated by the arrow) above the granulation tissue (scale bar: 250 μm).

a culture substratum could support the growth of epithelial cells [37]. In addition, techniques such as co-culture of two types of cells (i.e. epithelia and fibroblasts) [38] or transplant of the tracheal epithelial cell sheets can be employed to reduce airway stenosis [39]. Overall, for the reconstruction of large segment tracheal defects, the intact epithelial lining is essential to prevent bacterial colonization or infection. Therefore, our future work will focus on promoting a functional epithelial lining in the current design.

5. Conclusion

In this study, we demonstrated a bioreactor that could be applied to grow tissue-engineered trachea. The flow generated in the dynamic environment of the bioreactor could stimulate chondrocyte proliferation and matrix secretion. Furthermore, chondrocytes were aligned with the flow direction, and the morphology was similar to that observed in native tracheal cartilage. In animal experiments, tissue-engineered tracheal constructs could resist collapse without deformation during the implantation period. The granulation tissue overgrowth was observed in the lumen of the graft with a pseudostratified ciliated epithelium covering a large area of the granulation tissue. In summary, this study indicates that PCL stent combined with collagen type II scaffold in conjunction with rotation bioreactor may be applicable for making tissue-engineering trachea.

Acknowledgements

This work was supported by the National Health Research Institutes, and the National Science Council, Taiwan.

Appendix

Figures with essential color discrimination. The majority of figures in this article may be difficult to interpret in black and white. The full color images can be found in the on-line version, at doi:10.1016/j.biomaterials.2009.04.028.

References

[1] Kojima K, Vacanti CA. Generation of a tissue-engineered tracheal equivalent. Biotechnol Appl Biochem 2004;39:257–62. Review.
[2] Kojima K, Bonassar LJ, Ignotz RA, Syed K, Cortiella J, Vacanti CA. Comparison of tracheal and nasal chondrocytes for tissue engineering of the trachea. Ann Thorac Surg 2003;76(6):1884–8.
[3] Kim J, Suh SW, Shin JY, Kim JH, Choi YS, Kim H. Replacement of a tracheal defect with a tissue-engineered prosthesis: early results from animal experiments. J Thorac Cardiovasc Surg 2004;128(1):124–9.
[4] Yamashita M, Kanemaru S, Hirano S, Magrufov A, Tamaki H, Tamura Y, et al. Tracheal regeneration after partial resection: a tissue engineering approach. Laryngoscope 2007;117(3):497–502.
[5] Kojima K, Bonassar LJ, Roy AK, Mizuno H, Cortiella J, Vacanti CA. A composite tissue-engineered trachea using sheep nasal chondrocyte and epithelial cells. FASEB J 2003;17(8):823–8.
[6] Kojima K, Bonassar LJ, Roy AK, Vacanti CA, Cortiella J. Autologous tissue-engineered trachea with sheep nasal chondrocytes. J Thorac Cardiovasc Surg 2002;123(6):1177–84.
[7] Macchiarini P, Jungebluth P, Go T, Asnaghi MA, Rees LE, Cogan TA, et al. Clinical transplantation of a tissue-engineered airway. Lancet 2008;372(9655):2023–30.
[8] Lin CH, Su JM, Hsu SH. Evaluation of type II collagen scaffolds reinforced by poly(epsilon-caprolactone) as tissue-engineered trachea. Tissue Eng Part C Methods 2008;14(1):69–77.
[9] Williamson AK, Chen AC, Sah RL. Compressive properties and function–composition relationships of developing bovine articular cartilage. J Orthop Res 2001;19(6):1113–21.
[10] Waldman SD, Couto DC, Grynpas MD, Pilliar RM, Kandel RA. A single application of cyclic loading can accelerate matrix deposition and enhance the properties of tissue-engineered cartilage. Osteoarthr Cartil 2006;14(4):323–30.
[11] Lee CR, Grodzinsky AJ, Spector M. Biosynthetic response of passaged chondrocytes in a type II collagen scaffold to mechanical compression. J Biomed Mater Res A 2003;64(3):560–9.
[12] Davisson T, Kunig S, Chen A, Sah R, Ratcliffe A. Static and dynamic compression modulate matrix metabolism in tissue engineered cartilage. J Orthop Res 2002;20(4):842–8.
[13] Sucosky P, Osorio DF, Brown JB, Neitzel GP. Fluid mechanics of a spinner-flask bioreactor. Biotechnol Bioeng 2004;85(1):34–46.
[14] Ohyabu Y, Kida N, Kojima H, Taguchi T, Tanaka J, Uemura T. Cartilaginous tissue formation from bone marrow cells using rotating wall vessel (RWV) bioreactor. Biotechnol Bioeng 2006;95(5):1003–8.
[15] Williams KA, Saini S, Wick TM. Computational fluid dynamics modeling of steady-state momentum and mass transport in a bioreactor for cartilage tissue engineering. Biotechnol Prog 2002;18(5):951–63.
[16] Saini S, Wick TM. Concentric cylinder bioreactor for production of tissue engineered cartilage: effect of seeding density and hydrodynamic loading on construct development. Biotechnol Prog 2003;19(2):510–21.
[17] Saini S, Wick TM. Effect of low oxygen tension on tissue-engineered cartilage construct development in the concentric cylinder bioreactor. Tissue Eng 2004;10(5–6):825–32.
[18] Dunkelman NS, Zimber MP, Lebaron RG, Pavelec R, Kwan M, Purchio AF. Cartilage production by rabbit articular chondrocytes on polyglycolic acid scaffolds in a closed bioreactor system. Biotechnol Bioeng 1995;46(4):299–305.
[19] Vunjak-Novakovic G, Martin I, Obradovic B, Treppo S, Grodzinsky AJ, Langer R, et al. Bioreactor cultivation conditions modulate the composition and mechanical properties of tissue-engineered cartilage. J Orthop Res 1999;17(1):130–8.
[20] Daniel H, Josette B, Jean CB. Biochemical and physicochemical characterization of pepsin-solubilized type II collagen from bovin articular cartilage. Biochem J 1997;161:303–12.
[21] Freshney RI. Culture of animal cells: a manual of basic technique. 3rd ed. New York: Wiley-Liss; 1994. p. 331–2.
[22] Kim YJ, Sah RY, Doong JY, Grodzinsky AJ. Fluorometric assay of DNA in cartilage explants using Hoechst 33258. Anal Biochem 1988;174(1):168–76.
[23] Enobakhare BO, Bader DL, Lee DA. Quantification of sulfated glycosaminoglycans in chondrocyte/alginate culture, by use of 1,9-dimethylmethylene blue. Anal Biochem 1996;243(1):189–91.
[24] Bergman M, Loxley R. Two improved and simplified methods for the spectrophotometric determination of hydroxyproline. Anal Biochem 1961;25(12):1961–5.
[25] Pörtner R, Nagel-Heyer S, Goepfert C, Adamietz P, Meenen NM. Bioreactor design for tissue engineering. J Biosci Bioeng 2005;100(3):235–45.
[26] Bilgen B, Sucosky P, Neitzel GP, Barabino GA. Flow characterization of a wavy-walled bioreactor for cartilage tissue engineering. Biotechnol Bioeng 2006;95(6):1009–22.
[27] Hwang YS, Cho J, Tay F, Heng JY, Ho R, Kazarian SG, et al. The use of murine embryonic stem cells, alginate encapsulation, and rotary microgravity bioreactor in bone tissue engineering. Biomaterials 2009;30(4):499–507.
[28] Janssen FW, Oostra J, Oorschot A, van Blitterswijk CA. A perfusion bioreactor system capable of producing clinically relevant volumes of tissue-engineered bone: in vivo bone formation showing proof of concept. Biomaterials 2006;27(3):315–23.
[29] Sun T, Norton D, Haycock JW, Ryan AJ, MacNeil S. Development of a closed bioreactor system for culture of tissue-engineered skin at an air–liquid interface. Tissue Eng 2005;11(11–12):1824–31.
[30] Nieponice A, Soletti L, Guan J, Deasy BM, Huard J, Wagner WR, et al. Development of a tissue-engineered vascular graft combining a biodegradable scaffold, muscle-derived stem cells and a rotational vacuum seeding technique. Biomaterials 2008;29(7):825–33.
[31] Smith RL, Donlon BS, Gupta MK, Mohtai M, Das P, Carter DR, et al. Fluid-induced shear on articular chondrocyte morphology and metabolism in vitro. J Orthop Res 1995;13(6):824–31.
[32] Lane Smith R, Trindade MC, Ikenoue T, Mohtai M, Das P, Carter DR, et al. Effects of shear stress on articular chondrocyte metabolism. Biorheology 2000;37(1–2):95–107.
[33] Chen HC, Lee HP, Sung ML, Liao CJ, Hu YC. A novel rotating-shaft bioreactor for two-phase cultivation of tissue-engineered cartilage. Biotechnol Prog 2004;20:1802–9.
[34] Gemmiti CV, Guldberg RE. Fluid flow increases type II collagen deposition and tensile mechanical properties in bioreactor-grown tissue-engineered cartilage. Tissue Eng 2006;12(3):469–79.
[35] Sondrup C, Liu Y, Shu XZ, Prestwich GD, Smith ME. Cross-linked hyaluronan-coated stents in the prevention of airway stenosis. Otolaryngol Head Neck Surg 2006;135(1):28–35.
[36] Teramachi M, Nakamura T, Yamamoto Y, Kiyotani T, Takimoto Y, Shimizu Y. Porous-type tracheal prosthesis sealed with collagen sponge. Ann Thorac Surg 1997;64(4):965–9.
[37] Risbud M, Endres M, Ringe J, Bhonde R, Sittinger M. Biocompatible hydrogel supports the growth of respiratory epithelial cells: possibilities in tracheal tissue engineering. J Biomed Mater Res 2001;56(1):120–7.
[38] Kobayashi K, Nomoto Y, Suzuki T, Tada Y, Miyake M, Hazama A, et al. Effect of fibroblasts on tracheal epithelial regeneration in vitro. Tissue Eng 2006;12(9):2619–28.
[39] Yang J, Yamato M, Shimizu T, Sekine H, Ohashi K, Kanzaki M, et al. Reconstruction of functional tissues with cell sheet engineering. Biomaterials 2007;28(34):5033–43.